Original Research Article

Electrochemical determination of inorganic mercury (II) on a poly(Eriochrome blue black R) modified carbon paste electrode

ABSTRACT

In this work a new, simple, fast, and efficient electrochemical approach for the determination of inorganic mercury (Hg^{2+}) using the differential pulse anodic stripping voltammetry (DPASV) technique was presented. This is achieved by modifying the surface of a carbon paste by electropolymerization of Eriochrome blue black R. First, the behavior of Hg^{2+} on the modified electrode is studied by cyclic voltammetry and electrochemical impedance spectroscopy, with a view to evaluate performance and understand the phenomena that take place on its surface. After, DPASV is used to optimize sensor in $HClO_4$ medium. The values obtained after optimization were excellent because a linear calibration graph was obtained in the concentration range of $1\ 10^{-9}$ to $9\ 10^{-9}$ M with correlation coefficient R^2= 0.9975%, the LOD and the LOQ obtained are respectively $3.23\ 10^{-10}$ M and $1.07\ 10^{-9}$ M. The relative standard deviation for 7 measurements (RSD) is 3.07%, which proves that this sensor is reproducible. Finally, this method has been successfully applied in real samples of water and the results obtained are satisfactory because the recovery rates of Hg^{2+} vary from 99.2 to 100.1%.

Keywords: Carbon paste electrode, poly(Eriochrome blue black R), inorganic mercury(II), differential pulse anodic stripping voltammetry.

1. INTRODUCTION

Mercury (Hg) is one of the representative heavy metals, ranked third on the list of toxicological dangerous substances by the United States Toxicology and Disease Registry [**Error! Reference source not found.**]. Hg is emitted into the environment and released into landfill and water systems from anthropogenic activities or natural sources [**Error! Reference source not found.**]. However, anthropogenic actions such as inappropriate industrial waste management and illegal artisanal gold mining resulted in Hg contamination of ecosystems and became a public health concern [**Error! Reference source not found.**]. So, humans and animals will be caused acute or chronic exposure through the intake of food and water [**Error! Reference source not found.**]. Species of Hg determine its environmental transport, bioavailability, and toxicity [**Error! Reference source not found.**]. The mercury inorganic (Hg^{2+}) species is the dominate form of mercury in water. The exposure of Hg^{2+} directly damages the human brain, nervous system, kidney, and endocrine system [**Error! Reference source not found.**]. Inorganic mercury tends to accumulate in the kidney, leading to renal failure [**Error! Reference source not found.**]. Similarly, exposure to inorganic mercury has been shown to disrupt the reproductive system and induces testicular immunosuppression and fibrosis via inhibition of the CD74 (antigen) signaling pathway in male mice [**Error! Reference source not found.**].

The global issue of Hg has begun to be confronted by the adoption of the Minamata Convention, which entered into force in 2017 under the auspices of UNEP (United Nation Environmental Protection) to reduce human and ecosystem Hg exposure [**Error! Reference source not found.**]. For this reason, the acceptable limit of inorganic mercury Hg(II) in drinking water has been set by the World Health Organization (WHO) and the US Environmental Protection Agency (EPA) as 30 nM and 10 nM, respectively [**Error! Reference source not found.**]. Therefore, there is a great desire to design reliable methods that are sensitive, selective and efficient for the determination of Hg^{2+}, especially in water. Many

analytical methods have been proposed, which including HPLC-ICP-MS [**Error! Reference source not found.**], non-chromatography atomic spectroscopy [**Error! Reference source not found.**], fluorescence sensing [**Error! Reference source not found.**], surface-enhanced Raman scattering [**Error! Reference source not found.**]. Although these methods show excellent detection performance, most of them require expensive precision instruments, complex sample preparation processes, skilled operators and cannot be conveniently used online or outdoors [**Error! Reference source not found.**]. To overcome these limitations, attention has turned to voltammetry, in particular differential pulse anodic stripping voltammetric (DPASV) due to its ability to achieve high sensitivity and selectivity. Additionally, it is user-friendly, allows rapid analysis, and is relatively inexpensive and highly suitable for in situ applications [**Error! Reference source not found.**]. Several materials have been used for the modification of the surface of the working electrode. Emerging polymers are generally believed to be signal enhancers in electroanalytical operations as a result of the respective prominent characteristics such as higher conductivity, lighter weight, more flexibility, simplified procurement and greater active sites as well as stronger adherence to the surface of the electrodes [**Error! Reference source not found.**]. Thus, several polymers have been investigated for the modification of the surface of the carbon paste electrode (CPE) by DPASV for the detection of Hg^{2+}. These include poly(2,2'-dithiodianiline) [**Error! Reference source not found.**], poly(Eriochrome black T) [**Error! Reference source not found.**, **Error! Reference source not found.**], polyglicine [**Error! Reference source not found.**], Poly(3-hexylthiophene) [**Error! Reference source not found.**], poly(3,4-ethylenedioxythiohene) nanorods/graphene oxide [**Error! Reference source not found.**].

In this paper we report a construction of a new chemically modified CPE for the determination of Hg^{2+} in aqueous medium. Eriochrome blue black R (Calcon) dye was used to form a film polymer in a basic medium for the modification of the surface of CPE by DPASV. The optimization of the operating analytical parameters, such as polymer concentration, solution and concentration of the supporting electrolyte, potential and time deposit, stirring of solution, and some differential pulse voltammetry parameters were studied. In addition, to evaluate the metrological performances, calibration plot, limit of detection, limit of quantification and interfering ions are investigated. Finally, the analytical application on real samples focused on well water.

2. EXPERIMENTAL PART

2.1. Apparatus

Electrochemical experiments were carried out with Palmsens potentiostat (Palm Instrument BV) connected by a laptop and the software PS trace Master 4 was used for the execution of command. A conventional three-electrode system was used throughout. The working electrode was a bare CPE or a poly(Eriochrome blue back R)-CPE, the counter electrode was a platinum wire and a silver-silver chloride electrode (Ag/AgCl) was employed as reference electrode.

2.2. Reagents and material

All chemicals used for the preparation of the stock and standard solutions were analytical grade. Graphite powder (99.9995%) was purchased by Alfa Aesar. Paraffin oil, Eriochrome blue black R, ($C_{20}H_{13}N_2NaO_5S$, scheme 1) were obtained from Sigma-Aldrich. The last one was prepared by dissolving the required amount in absolute ethanol. Stock solutions 10^{-2} mol.L^{-1} of Hg^{2+} were prepared from mercury chloric $HgCl_2$, (Merck KGaA) in 0.1 mol.L^{-1} of $HClO_4$ solution. More diluted mercury standards were prepared from this solution. Some ions used in interference studies Pb^{2+}, Cd^{2+}, Cu^{2+}, Cl^- and CN^- were prepared respectively from lead chloride, $Pb(Cl)_2$ (Merck Schuchardt OHG); zinc chloric, $Zn(Cl)_2$ (Alfa Aesar); cadmium chloride, $Cd(Cl)_2$ (Alfa Aesar); copper chloride, $Cu(Cl)_2$ (Alfa Aesar); potassium chloride, KCl (Merck KGaA) and potassium cyanide, KCN (Merck KGaA).

2.3. Sample preparation

Tap water samples were collected from the laboratory. The well water sample was collected in the city of Niamey (Capital of Niger).

2.4. Preparation of carbon paste electrode

The bare CPE was prepared by mixing 2 g of graphite powder and 0.76 mL of paraffin oil in a mortar using a pestle. The mixture was carried out until a homogenous paste was obtained. Once homogeneity was observed, the mixed paste was then inserted into the cylindrical cavity of the CPE and polished on smooth paper.

2.5. Electropolymerization of the monomer on carbon paste electrode

As it has been reported by Geng and Hu [21], electropolymerization is more favorable in alkaline medium for the deposition than acidic because of the large amount of proton loss in acidic medium. So, the electropolymerization of Eriochrome Blue Black R (EBB R) was done similarly to literature [16]. It was carried out in 0.1 mol.L^{-1} NaOH solution containing 3. 10^{-4} mol.L^{-1} Eriochrome blue black R by cyclic voltammetry. The potential was scanned between - 0.4 and +1 V at a sweep rate of 100 mV.s^{-1} for 25 cycles.

2.6. Differential pulse anodic stripping voltammetric (DPASV) measurement of Hg^{2+} at the modified electrode

The poly(EBB R)-CPE was immersed in aqueous solution containing a selected concentration of Hg^{2+} in 0.1 mol.L^{-1} KCl. The preconcentration of Hg^{2+} was carried out under open circuit and in stirred solution. After the preconcentration step was completed, stirring was stopped and a 30 s rest period was allowed for the solution to become quiescent. Then the voltammogram was scanned from -0.4 V to 1 V using DPASV. The parameters of differential pulse voltammetry used were a potential step height of 10 mV, pulse amplitude of 50 mV and duration of 50 ms. The same procedure was used for bare CPE and poly(EBB R)-CPE.

3. RESULTS AND DISCUSSION

3.1. Electropolymerization of Eriochrome blue black R (EBB R) on the surface of carbon paste electrode

The cyclic voltammograms during the electropolymerization of Eriochrome blue black R were shown in Fig. 1. Eriochrome blue black R was electropolymerized on the working electrode surface by scanning the potential from -0.4 to 1 V at a scan rate of 100 mV.s^{-1} for 25 cycles in 0.1 mol.L^{-1} NaOH. During the first scan, a well-defined anodic peak (Pa_1) and cathodic peak (Pc_1) were observed at -0.02 V/0.394 µA and -0.07 V/ -0.137 µA, respectively. These peaks show that there is an exchange of electrons at the interface electrode/electrolyte. The anodic peak is due to the oxidation of the monomer which initiates the polymerization [21]. From the 1st scan to the 2nd scan, there is a large drop in the intensity of the anodic peak. The anodic and cathodic peaks decrease gradually during successive scans, and tend to become stable after 25 scans. Guha et al. [16] and Yao et al. [17], made the same observation during the electropolymerization of Eriochrome black T, and reported that such a decrease indicates the formation and deposition of the polymer film on the surface of the electrode. Eriochrome blue black R, like other dyes, are very electron-rich compounds. Therefore, it is complicated to present a rather detailed mechanism for the electropolymerization of the latter. Thus, in the literature the authors limit themselves to a simple mechanism. Based on what Guha et al. [16] and Yao et al. [17], reported, the polymerization of EBB R structure (a, Scheme 1) follows the formation of benzoquinone diimine structure (b, Scheme 1) which is then reduced back to EBB R on the surface of the electrode. The mechanism is shown in Scheme 1.

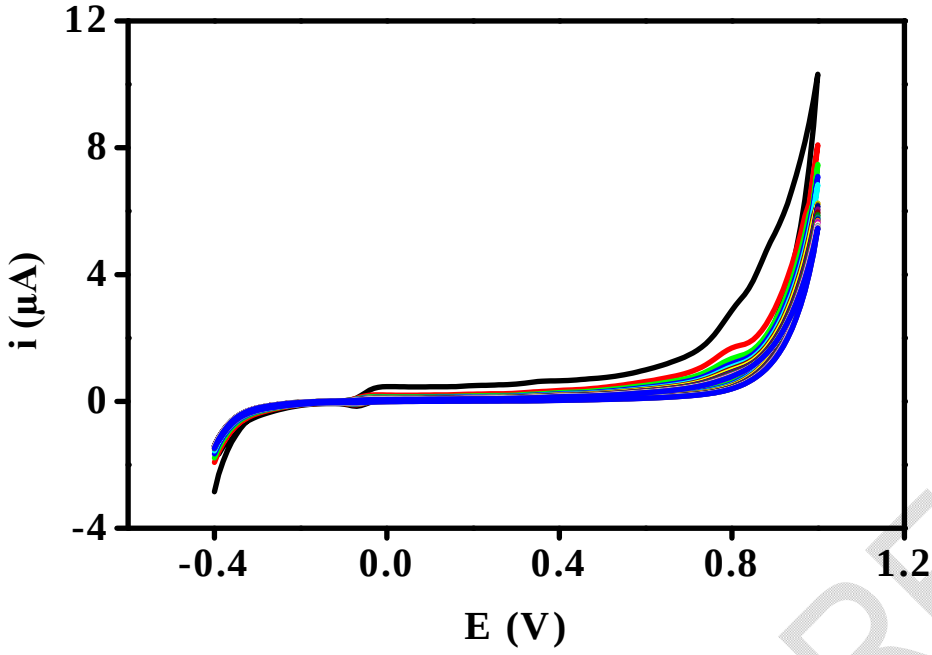

Fig. 1. Cyclic voltammograms recorded for the polymerization of Eriochrome blue black R at the carbon paste electrode in 0.1 M of NaOH containing 300 µM of monomer during 25 cycles. Scan rate, 100 mV.s^{-1}

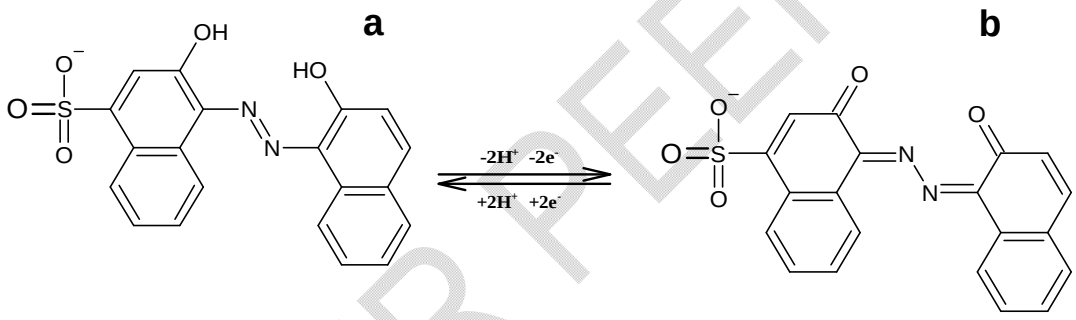

Scheme 1. Mechanism of polymerization of Eriochrome blue black R

3.2. Characterization by electrochemical impedance spectroscopy (SIE)

The surface morphology of CPE-modified with poly(EBB R) was characterized by SIE. The Nyquist plots of the bare carbon paste electrode (black curve) and the carbon paste electrode modified with poly(EBB R) (red curve) in the supporting electrolyte of 1 M KCl containing 1 mM of the complex $[Fe(CN)6]^{3-/4-}$ are shown in Fig. 2. The two curves describe a semicircle and a straight line. In general, the semicircle in the higher frequency is characteristic of the highest charge transfer resistance and the straight line in low frequency is due to the diffusion limiting process [22]. We note that the charge transfers resistance (Rct) of the bare carbon paste electrode and the carbon paste electrode modified with poly(EBB R) are 15 kΩ and 5 kΩ, respectively. According to Salih et al. [23], the decrease in the Rct observed during the modification of the poly(EBB R) modified-CPE shows that the polymer (poly(EBB R)) was effectively carried out and significantly increase the electron transfer at the electrode surface because of the electronic properties of the polymer.

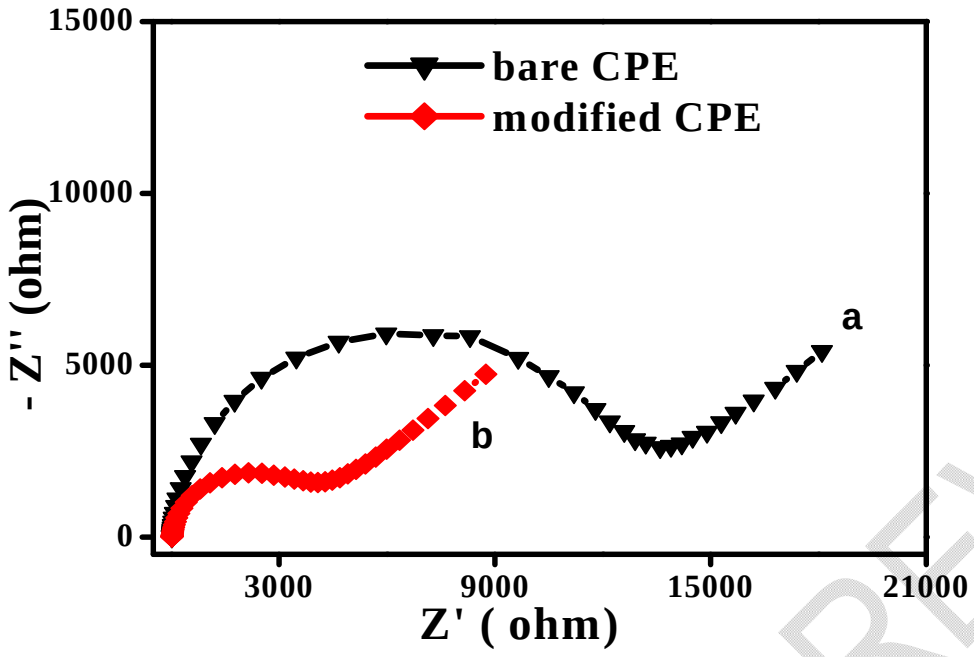

Fig. 2. Nyquist plots for different electrodes in 1 mM of $[Fe(CN)6]^{3-/4-}$ containing 1 M KCl: a. bare carbon paste electrode; b. modified poly(EBB R)-carbon paste electrode

3.3. Electrochemical behavior of Hg(II) ions at the bare carbon paste and modified poly(Eriochrome blue black R)-carbon paste electrode

3.3.1. Characterization by cyclic voltammetric

Cyclic voltammograms of bare CPE and modified poly(EBB R)-CPE in 1 M KCl for the detection of 2.5 10^{-4} M of $Hg^{2+}$are illustrated in Fig. 3. It can be seen that no peak (green curve) is displayed at the bare CPE in the absence of Hg^{2+}. But in the presence of Hg^{2+} (red curve) a weak peak anodic 0.070 V/6.25 µA is observed then a crossing between the anodic branch and cathodic branch. Moreover, when the modified poly(EBB R)-CPE is immersed in the solution in presence of Hg^{2+} (black curve) a high peak 0.070 V/20.38 µA was observed, which was more intense than the bare CPE, then two crossing between the anodic and cathodic branch's. The bare CPE has the difficulty of preconcentration the Hg^{2+} in the solution while the modified CPE by the film polymer significantly increased the intensity of the current, showing easier charge transfer on the surface of the polymer film.

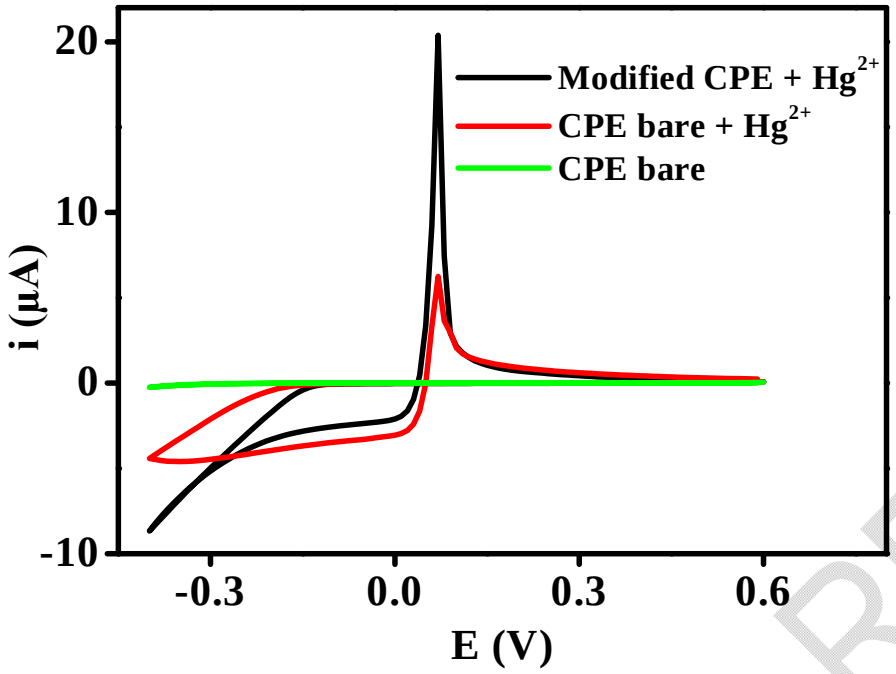

Fig. 3. Cyclic voltammograms obtained at: a. bare CPE, b. bare CPE containing 2.5 10^{-4} M Hg^{2+} and c. poly(EBB R)-CPE containing 2.5 10^{-4} M Hg^{2+} in 1 M KCl; Scan rate 50 mV/s

3.3.2. Determination of Hg2+ by differential pulse anodic stripping voltammetry

Preliminary studies of mercury accumulation were carried out by recording the Differential Pulse Anodic Stripping Voltammograms on a bare carbon paste electrode and on the MCPE.

Firstly, the study of the behavior of the bare carbon paste electrode and the modified polymer film-CPE in the supporting electrolyte 0.1 M KCl were illustrated in Fig. 4. It can be seen that no oxidation peak (black and blue curve) is displayed at the bare CPE and modified polymer film-CPE in the absence of Hg^{2+}. It proves that the solution isn't contaminated. Then, when Hg^{2+} was added in the same solution (0.1 M KCl) and under the same conditions at the bare CPE (green curve) and modified polymer film-CPE (red curve), an anodic pic was observed at 0.088 V/2.38 µA and 0.092 V/20.34 µA, respectively. These results show that the best response is that provided by the modified CPE, and it is 8.5 times more intense than the bare CPE. The peak is well resolved and will serve for the determination of inorganic mercury in aqueous medium. The following reaction may take place at the surface of the electrode [24]:

Step 1: (Preconcentration of Hg^{2+}) Hg^{2+} + poly(EBB R) → Hg^{2+}-poly(EBB R)-CPE
Step 2: (Reduction of Hg^{2+}) Hg^{2+}-poly(EBB R)-CPE + 2e- → Hg^{0} + poly(EBB R)-CPE
Step 3: (Redissolution of Hg^{2+}) Hg^{0} → Hg^{2+} + 2e-

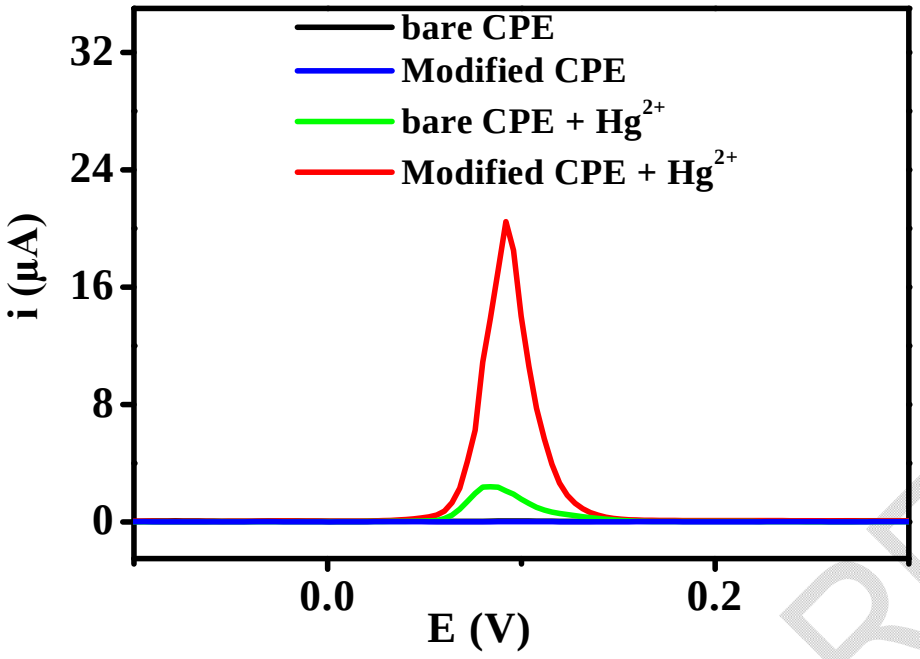

Fig. 4. DPASV of bare CPE (a), modified poly(EBB R)-CPE (b), bare CPE in the presence of 2.5 10^{-4}M Hg^{2+} (c), modified poly(EBB R)-CPE in presence of 2.5 10^{-}4 M Hg^{2+} (d), in 0.1 M KCl; scan rate 20 mV/s; deposition time 120 s; pulse amplitude 50 mV

3.4. Optimization of analytical parameters

3.4.1. Effect of concentration of Eriochrome blue black R

The effect of concentration of Eriochrome blue black R during the electropolymerization has been studied between 100 and 700 µM. As shown in Fig. 5, the intensity of the peak current of Hg^{2+} oxidation increase according to the concentration of EBB R from 100 µM to 350 µM. The increase in the intensity of the current is explained by the increase of monomer on the surface of carbon paste to form more polymer and therefore more sites capable to accumulate mercury (II). When increasing the concentration of EBB R beyond 350 µM, the sensitivity of mercury (II) determination by the modified poly(EBB R)-CPE decrease. According to several authors, such as Dueraning et al. [25], this was probably because the polymer became too thick and blocked the electrical conductivity. Moreover, there are some oxidation peaks appearing in cyclic voltammograms which lead us to the decrease in the intensity of the current. These new oxidation peaks could be

due to the appearance of new sites to capture the inorganic mercury present in the solution during the first step of

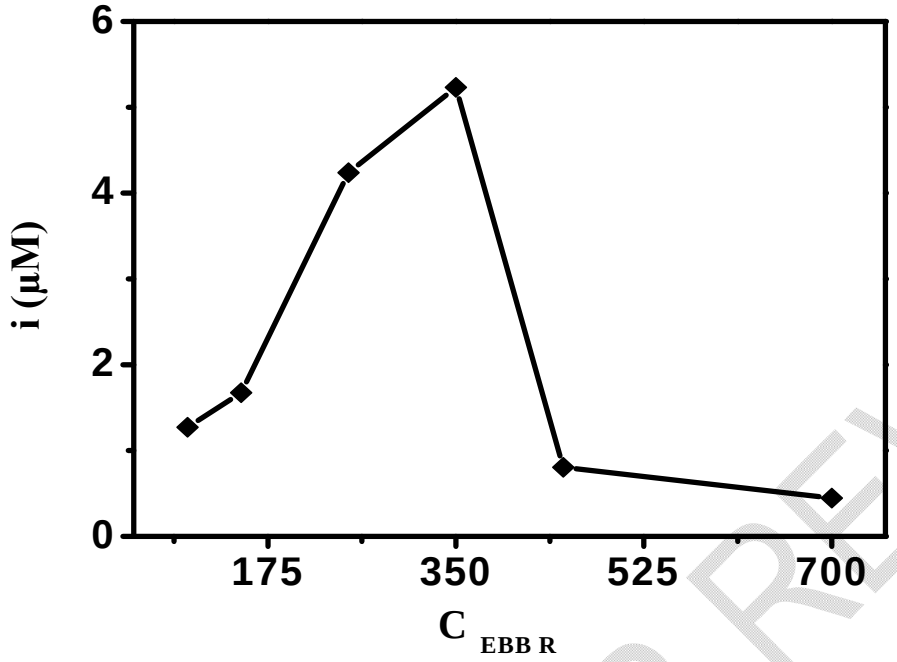

DPASV.

Fig. 5. Effect of the variation of the EBB R (Calcon) concentration on the peak current intensity by DPASV. [Hg^{2+}] 35 µM; scanning speed 20 mV/s; deposition time 120 s; pulse amplitude 50 mV

3.4.2. Effect of supporting electrolyte

The differential pulse voltammograms of 35 µM of Hg^{2+}, carried out in 0.1 M of KCl, NH_4Cl, KNO_3, KCl, NH_4Cl, acetate buffer solution (ABS) (pH=4.22) and phosphate buffer solution (PBS) (pH= 6.68), are illustrated in Fig. 6. The optimum response was observed in $HClO_4$ medium and this electrolyte was chosen as the supporting electrolyte for the remaining experiments. The high intensity of the current in $HClO_4$, is explained by the fact that it is an acid in which the mercury chloride ($HgCl_2$) has a high solubility, allowing it to have in solution, the specie Hg^{2+}.

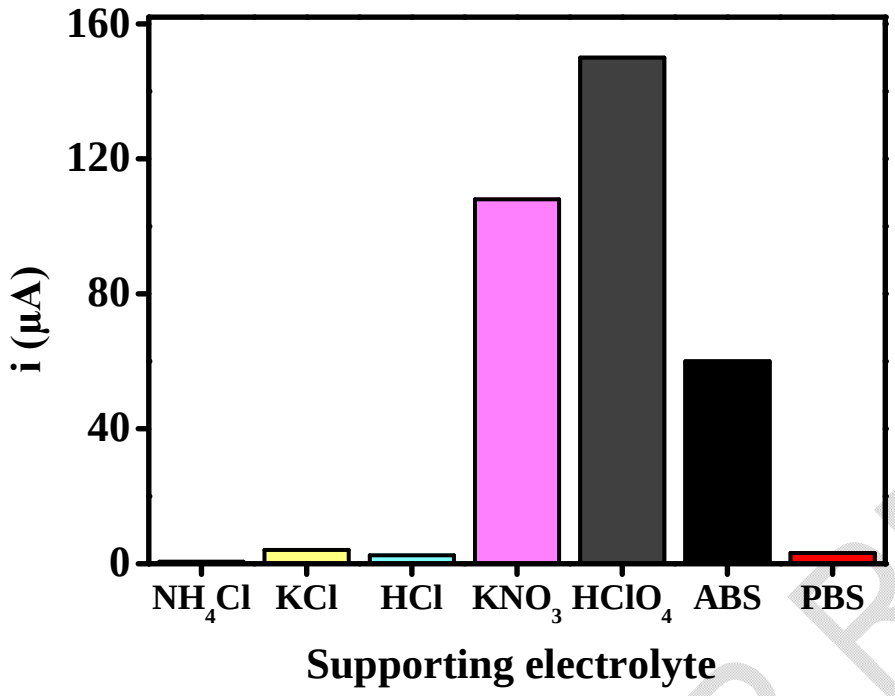

Fig. 6. Effect of supporting electrolyte on DPASV peak current for the determination of 35 μM Hg^{2+}

3.4.3. Effect of the concentration of supporting electrolyte

The effect of the concentration of $HClO_4$ has been studied. It can be seen in Fig. 7, that the intensity of the current increases depending on the concentration of the supporting electrolyte from 0.1 to 0.8 M, and after 0.8 M a decrease is observed. Therefore, 0.8 M of $HClO_4$ was used for further experiments.

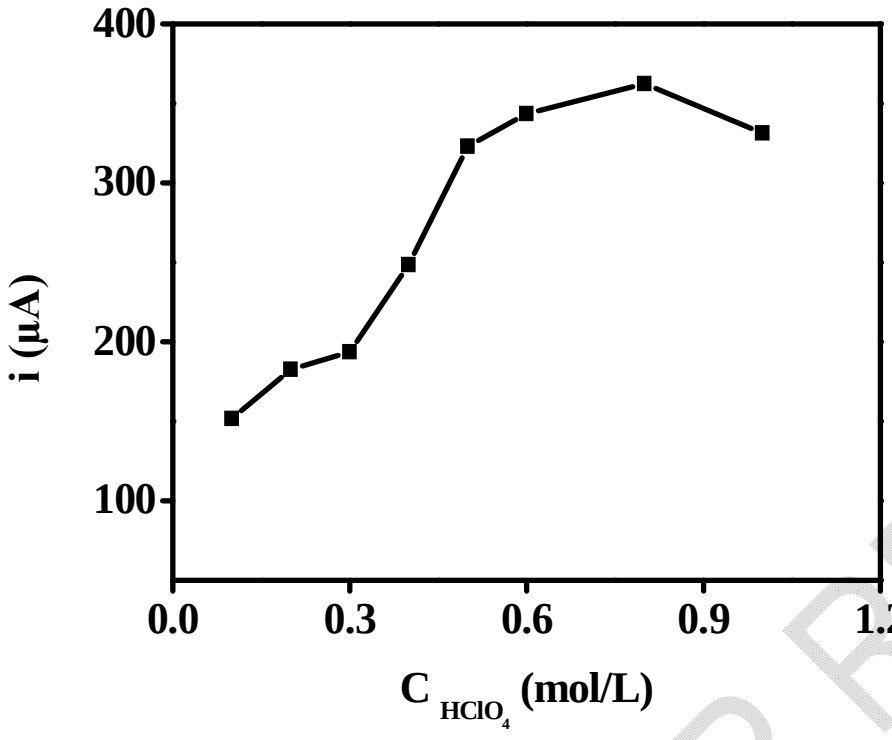

Fig. 7. Effect of concentration of HClO4 on DPASV peak current for the determination of 35 µM Hg^{2+}

3.4.4. Effect of deposition potential

Deposition potential is an important parameter for stripping techniques and has a significant effect on the sensitivity [26]. Fig. 8 shows a significant increase in intensity as a function of the deposition potential of the current down to -350 mV. Over this potential, the intensity of the peak decreases. So, the deposition potential of - 350 mV was taken as the optimal potential for mercury (II) deposition on the surface of the modified electrode.

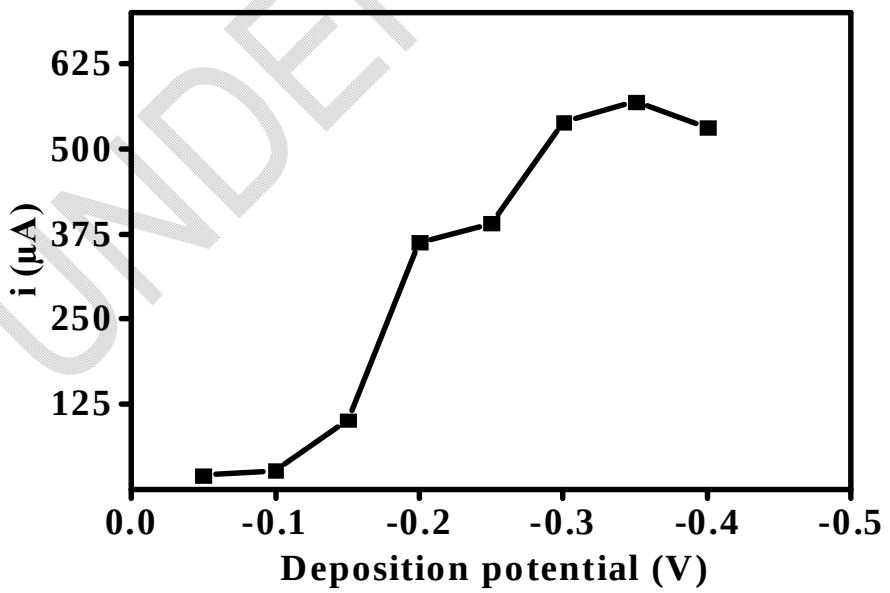

Fig. 8. Effect of the variation of the deposition potential on the peak current intensity by DPASV. [Hg^{2+}] 35 µM; scan rate 20 mV/s; pulse amplitude 50 mV; stirring speed 400 rpm

3.4.5. Effect of deposition time

Fig. 9 illustrated the effect of deposition time in the range of 0 to 240 s on the current intensity. It seen that the peak current increase with the deposition time from 0 to 120 s. while, the peak current was decreased with further the deposition potential up to 120 s. The decrease is due to the saturation of mercury inorganic on the surface of the electrode. Therefore, 120 seconds was chosen as optimal deposition time.

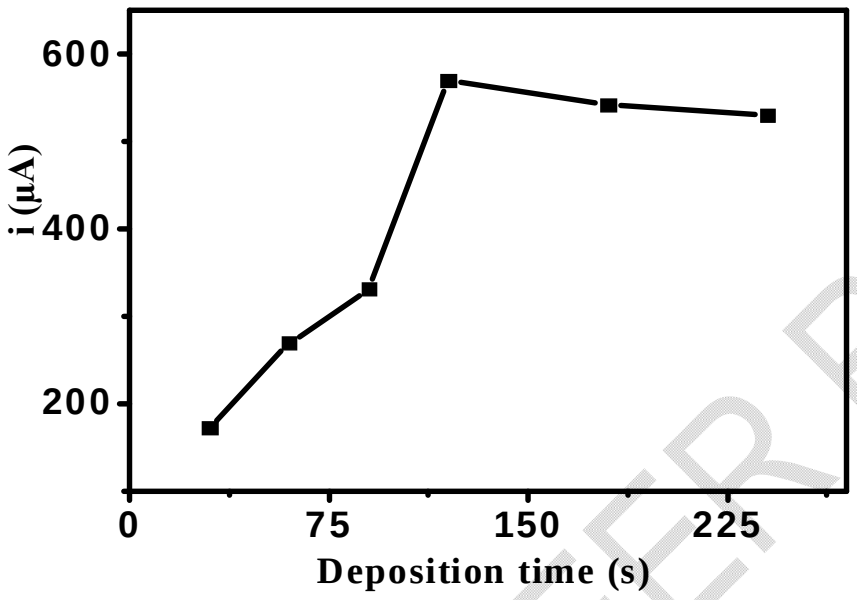

Fig. 9. Effect of the variation of the deposition time on the peak current intensity by DPASV. [Hg^{2+}] 35 µM; scan rate 20 mV/s; deposition potential -0,35V; pulse amplitude 50 mV; stirring speed 400 rpm

3.4.6. Effect of mechanical stirring of the solution

Stirring of a solution during voltammetric measurements will give an increase in signal due to a better mass transport to the electrode and corresponding to an effective decrease of the thickness of the diffusion layer [27]. Mechanical stirring speed, between 200 and 700 rpm (revolution per minutes), was applied in the mercury deposition step. Results are shown in Fig. 10. The intensity of the peak current increases linearly with the increase of the stirring speed up to 600 rpm, but dropped at 700 rpm. According to several authors such as [28], this decrease could be attributed to more distribution of the solution that could perturb the deposition step. At 600 rpm, the highest current peak is obtained, but 400 rpm was selected for further experiments because the best reproducibility of the measurements was found at this stirring speed.

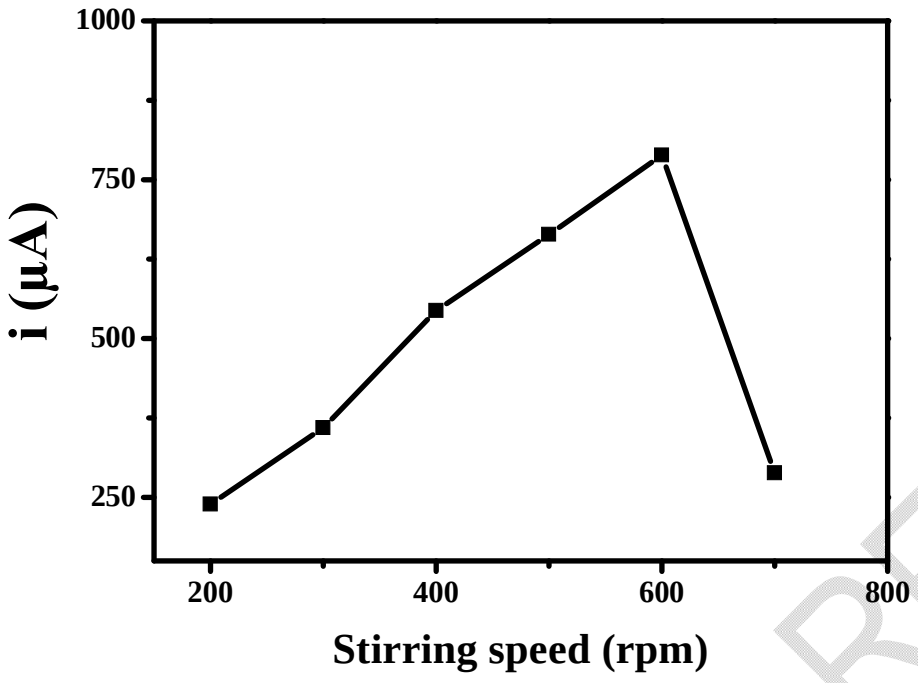

Fig. 10. Effect of mechanical stirring speed on peak current intensity by DPASV. [Hg^{2+}] 35 µM; scan rate 20 mV/s; deposition time 120 s; pulse amplitude 50 mV

3.4.7. Optimization of DPV parameters

The influence of various parameters of DPV such as potential step, pulse amplitude, pulse time and scan rate were investigated in order to achieve high sensitivity for trace Hg^{2+} determination with the modified electrode. The potential step was varied from 1 to 8 mV. As illustrated in Fig. 11.a, the maximum current intensity was found at 4 mV. Fig. 11.b shows the effect of the pulse amplitude on the current intensity in the range of 30 and 80 mV. The optimal pulse amplitude was at 80 mV. As shown in Fig. 11.c the variation of pulse time on the current intensity was studied from 10 to 50 ms. The optimal pulse time was found at 30 ms. Finally, for the variation of scan rate, investigated in Fig. 11.d, the optimal value was 20 $mV.s^{-1}$.

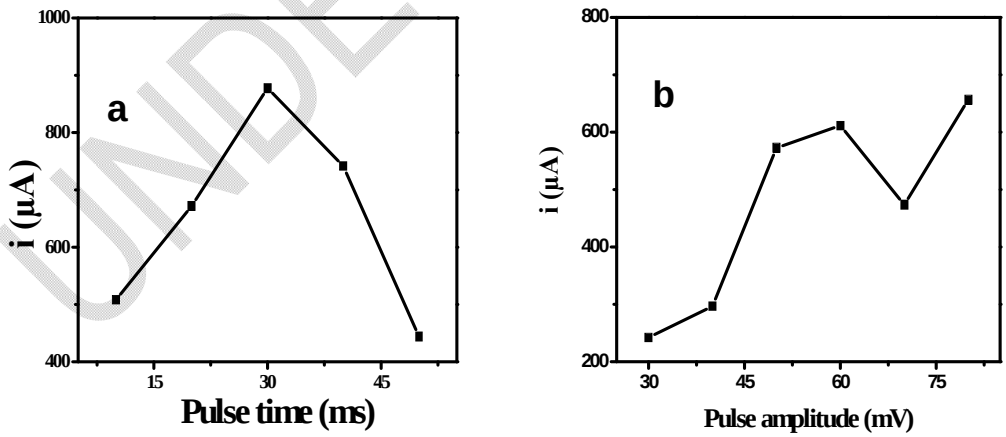

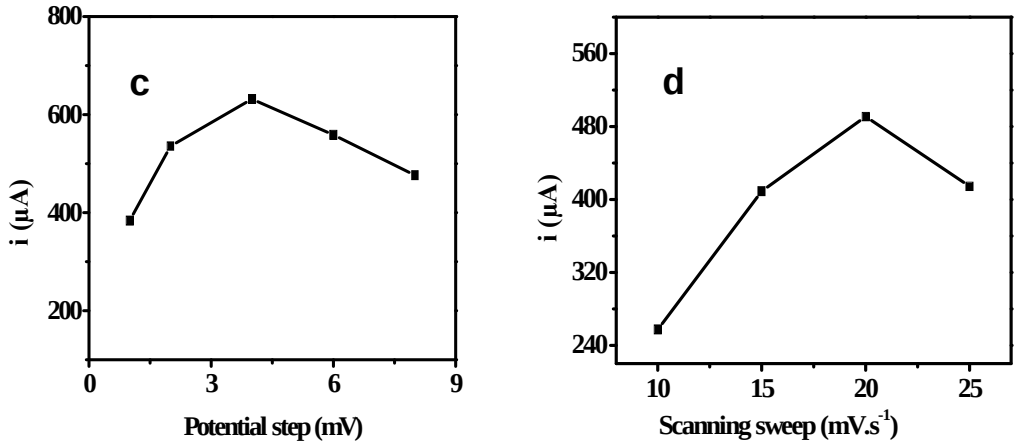

Fig. 11. Influence of DPV parameters (a. Pulse time; b. Pulse amplitude; c. Potential step; and d. Scanning sweep) on the peak current intensity by DPASV for determination of 35 µM Hg^{2+} in 0.8 M of $HClO_4$

3.4.8. Calibration plot

The Fig. 12 presents the differential pulse voltammograms of various concentration of Hg^{2+} in the range of 0 to 9 10^{-9} M, with the poly(EBB R)-CPE. It was observed that the peak currents increase linearly with the increased concentration of Hg^{2+} in the range studied, and the corresponding linear regression equation was Ipa (µA) =1.479 $10^{+8}[Hg^{2+}]$ – 0.00656 with a correlation coefficient (R^2) of 0.9987. The limit of detection (LOD) and the limit of quantification (LOQ), calculated in the concentration range of 1 10^{-9} to 9 10^{-9} M are respectively 3.23 10^{-10} M and 1.07 10^{-9} M. The relative standard deviation (RSD) for seven repetitions analysis in 0.8 M of $HClO_4$ containing 5 10^{-9} M Hg^{2+} by DPASV was 3.07 %.

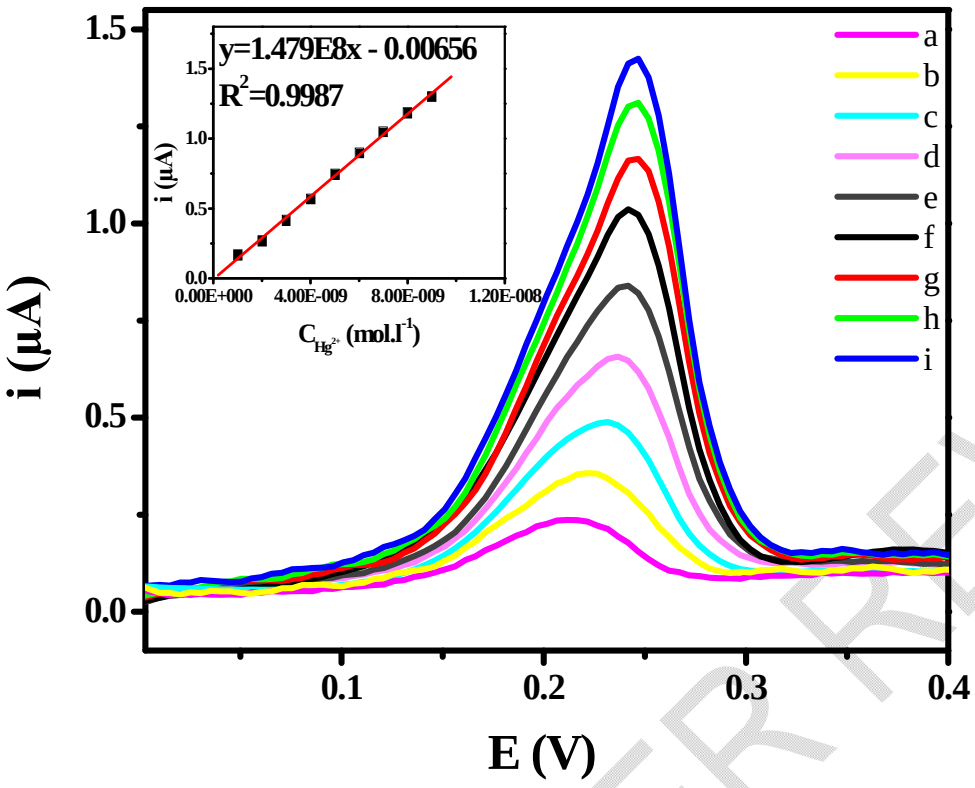

Fig. 12. DPASV of various concentrations of Hg^{2+} to 0 to 9 10^{-9} M: b) 1 10^{-9} M, c) 2 10^{-9} M, d) 3 10^{-9} M, e) 4 10^{-9} M, f) 5 10^{-9} M, g) 6 10^{-9} M, h) 7 10^{-9} M, i) 8 10^{-9} M, j) 9 10^{-9} M

Table 1 shows the comparison of the modified poly(Eriochrome blue black R)-CPE presented in this work with other electrodes reported in the literature for the detection of Hg^{2+}. This comparison is based on the relative standard deviation (RSD) and LOD of the different sensors. As can be seen in the Table 1, this method showed a low detection limit and satisfactory RSD. This proves that the sensor developed in this work is sensitive, efficient, and can be used for trace level analysis in aqueous media.

Table 1. Comparison of modified poly(Eriochrome blue black R)-CPE with other modified CPE developed for the determination of Hg^{2+}

Electrodes	Technique	LOD (M)	RSD	Accumulation time (s)	Reference
poly(Eriochrome blue black R)/CPE	DPASV	3.23 10^{-10}	3.07 % for 7 measurements	120	Present work
poly(Eriochrome black T)/CPE	DPASV	2.20 10^{-10}	2.4 % for 6 measurements	120	[**Error! Reference source not found.**]
poly(glycine)/GPE	DPV	6.60 10^{-6}	/	/	[**Error! Reference source not found.**]
EDTA/CPE	SWV	8.6 10^{-9}	3.1 % for 7 measurements	300	[**Error! Reference source not**

12-Crown Ether/MWCNTs/CPE	LS-AdSV	1.25 10^{-10}	5 % for 10 measurements	/	**found.**] [**Error! Reference source not found.**]
5-Br-PADAP/CPE	DPV	1 10^{-8}	1.6 % for 10 measurements	120	[**Error! Reference source not found.**] [**Error! Reference source not found.**]

3.4.9. Interference studies

In gold mining sites, are listed the presence of certain ions such as Cd^{2+}, Cu^{2+}, $Zn^{2+}Pb^{2+}$, CN^- and Cl^- which can affect the determination of inorganic mercury using CPE-modified with poly(Eriochrome blue black R). The presence of these ions was examined for the determination of 10^{-8} M Hg^{2+} using the optimal conditions described above. The experimental results illustrated at Table 2 show the response of the modified electrode is not remarkably disturbed but some ions such as CN^- interfere when they were 10 fold excess over Hg^{2+} in the analyte solution. For the CN^-, this could be due to his strong affinity towards Hg^{2+} at the surface of the electrode. The matrix effect is minimized, during measurements on real samples, using the standard addition technique.

Table 2. Interference of some ions with the determination of 10^{-8} mol.L^{-1} of Hg^{2+} at poly(EBB R)- CPE

	Current intensity (1 fold)	Current variation	Current intensity (10 fold)	Current variation
Hg^{2+}	0.3125 ± 0.06			
Cd^{2+}	0.3226 ± 0.03	+ 0.03 %	0.354 ± 0.05	+ 0.13%
Cu^{2+}	0.311 ± 0.01	- 0.004 %	0.276 ± 0.006	- 11.6%
Zn^{2+}	0.289 ± 0.05	- 7.3 %	0.282 ± 0.03	- 9.8%
CN^-	0.292 ± 0.009	- 6.4%	0.145 ± 0.01	- 53.4%
Cl^-	0.249 ± 0.04	- 3.42 %	0.423 ± 0.02	+ 35%
Pb^{2+}	0.345 ± 0.02	+ 10 %	0.415 ± 0.03	+ 32%

3.4.10. Analytical applications

In order to evaluate the analytical applicability of the proposed method, known concentrations of Hg was introduced into samples and determined by the standard addition method using the optimal parameters described. The results of the recovery data of different concentrations in distilled water and well water obtained (Table 3) are between 98.71 and 100.38% which are very satisfactory. Thus, The sensor poly(EBB R)-CPE developed is very suitable for the determination of trace of mercury (II) ions in aqueous media.

Table 3. Recovery data for Hg2+ obtained for distilled water and well water

Samples	[Hg^{2+}] Spiked (µM)	[Hg^{2+}] Founded (µM)	Recovery (%)
Distilled water	0.002	0.00198	98.76
	0.005	0.005019	100.38
	0.0075	0.007404	98.71
Well water	0.005	0.00496	99.2
	0.05	0.05005	100.1

4. CONCLUSION

In this work, we reported a new sensitive and efficient sensor using modified with poly(Eriochrome blue black R)-CPE for the determination of Hg^{2+} in aqueous medium. Cyclic voltammetry and electrochemical impedance spectroscopy show a well deposited film polymer on the surface of carbon paste. After optimization of analytical parameters, the sensor has a linear dynamic range, a low limit of detection, a good reproducibility and application of this sensor in real samples were satisfactory.

REFERENCES

1. Liao Y, Li J, Li S, Han B, Wu P, Deng N et al. Inorganic mercury induces liver oxidative stress injury in quails by inhibiting Akt/Nrf2 signal pathway, Inorg. Chem. Commun. 2022; 142: 109603. DOI: https://doi.org/10.1016/j.inoche.2022.109603
2. Ganguly J, Kulshreshtha D, Jog M. Mercury and Movement Disorders: The Toxic Legacy Continues. *Can. J. Neurol. Sci*. 2022;49 :493 – 501. DOI: https://doi.org/10.1017/cjn.2021.146
3. Nunes PBdO, Ferreira MKM, Frazão DR, Bittencourt LO, Chemelo VdS., Silva MCF et al. Effects of inorganic mercury exposure in the alveolar bone of rats: an approach of qualitative and morphological aspects. *PeerJ*. 2022;10 :12573. DOI: https://1.doi.org/10.7717/peerj.12573
4. Li S, Han B, Wu P, Yang Q, Wang X, Li J et al. Effect of inorganic mercury exposure on reproductive system of male mice: Immunosuppression and fibrosis in testis, *Environ. Toxicol*. 2022;37: 69-78. DOI: https://onlinelibrary.wiley.com/doi/epdf/10.1002/tox.23378
5. Han B, Lv Z, Han X, Li S, Han B, Yang Q et al. Harmful Effects of Inorganic Mercury Exposure on Kidney Cells: Mitochondrial Dynamics Disorder and Excessive Oxidative Stress. *Biol. Trace Elem. Res*. 2022;200:1591–1597. DOI: https://doi.org/10.1007/s12011-021-02766-3
6. Tian J, Zhu Y. Rapid Determination of Mercury Ions in Environmental Water Based on an N-Rich Covalent Organic Framework Potential Sensor. *Int. J. Chem. Eng.* 2022;2022:3112316. DOI: https://1.doi.org/10.1155/2022/3112316
7. Cossa D, Knoery J, Bănaru D, Harmelin-Vivien M, Sonke JE, Hedgecock IM et al. Mediterranean Mercury Assessment 2022: An Updated Budget, Health Consequences, and Research Perspectives. *Environ. Sci. Technol*. 2022;56(7): 3840–3862. DOI: https://doi.org/10.1021/acs.est.1c03044
8. Che S, Yin L, Fan Y, Shou Q, Zhou C, Fu H, She Y. An ionic liquid-based ratio fluorescent sensor for real-time visual monitoring of trace Hg^{2+}. *Sens. Actuators B Chem*. 2022;360(1):131588. DOI: https://doi.org/10.1016/j.snb.2022.131588
9. Wang Y, Zhu A, Fang Y, Fan C, Guo Y, Tan Z, et al. Dithizone-functionalized C18 online solid-phase extraction-HPLC-ICP-MS for speciation of ultra-trace organic and inorganic mercury in cereals and environmental samples. *J. Environ. Sci.* 2022;115:403–410. DOI: https://doi.org/10.1016/j.jes.2021.08.013
10. Yang H, Jian R, Liao J, Cui J, Fang P, Zou Z, Huang K. Recent development of non-chromatographic atomic spectrometry for speciation analysis of mercury. *Appl. Spectrosc. Rev.* 2021;57:441-460 DOI: https://doi.org/10.1080/05704928.2021.1893183
11. Ali S, Mansha M, Baig N, Khan SA. Cost-Effective and Selective Fluorescent Chemosensor (Pyr-NH@SiO2 NPs) for Mercury Detection in Seawater. *Nanomaterials*. 2022;12:1249. DOI: https://doi.org/10.3390/nano12081249
12. Liu Q, Wu F, Di H, Bi Y, Meng M, Liu D et al. A novel SERS biosensor for ultrasensitive detection of mercury(II) in complex biological samples. *Sens. Actuators B Chem*. 2022;351:130934. DOI: https://doi.org/10.1016/j.snb.2021.130934
13. Mahamane AA, Despas C, Adamou R, Walcarius A. Carbon paste electrode modified with 5-Br-PADAP as a new electrochemical sensor for the detection of inorganic mercury(II). *J. Mater. Environ. Sci*., 2022;13(01):54-69. https://www.jmaterenvironsci.com/Document/vol13/vol13_N1/JMES-2022-13005-Mahamane.pdf
14. Tajik S, Beitollahi H, Nejad FG, Dourandish Z, Khalilzadeh MA, H. W. Jang et al. Recent Developments in Polymer Nanocomposite-Based Electrochemical Sensors for Detecting Environmental Pollutants. *Ind. Eng. Chem. Res*. 2021;60(03):1112−1136. DOI: https://doi.org/10.1021/acs.iecr.0c04952
15. Somerset V, Leaner J, Mason R, Iwuoha E, Morrin A. Development and application of a poly(2,2′-dithiodianiline) (PDTDA)-coated screen-printed carbon electrode in inorganic mercury determination. Electrochim. Acta. 2010;55 (14):4240-4246. DOI: https://doi.org/10.1016/j.electacta.2009.01.029
16. Guha KS, Mascarenhas RJ, Thomas T, D'Souza OJ. Differential pulse anodic stripping voltammetric determination of Hg^{2+} at poly(Eriochrome Black T)-modified carbon paste electrode. *Springer*. 2014;20:849–856. DOI: https://doi.org/10.1007/s11581-013-1040-9
17. Yao H, Sun Y, Lin X, Tang Y, Liu A, Li G et al. Selective Determination of Epinephrine in the Presence of Ascorbic Acid and Uric Acid by Electrocatalytic Oxidation at Poly(eriochrome Black T) Film-modified Glassy Carbon Electrode. *Anal. Sci*. 2007;23 (6):677-682. DOI: https://doi.org/10.2116/analsci.23.677

18. Raril C, Manjunatha JG. Fabrication of novel polymer-modified graphene-based electrochemical sensor for the determination of mercury and lead ions in water and biological samples. *J. Anal. Sci. Technol*. 2020;11:3. DOI: https://doi.org/10.1186/s40543-019-0194-0
19. Tamer U, Oymak T, Ertas N. Voltammetric Determination of Mercury(II) at Poly(3-hexylthiophene) Film Electrode. Effect of Halide Ions. *Electroanalysis*. 2007;19:2565 – 2570. DOI: https://doi.org/10.1002/elan.200704013
20. Zuo Y, Xua J, Zhua X, Duana X, Lub L, Gaoa Yet al. Poly(3,4-ethylenedioxythiophene) nanorods/graphene oxide nanocomposite as a new electrode material for the selective electrochemical detection of mercury (II). *Synth. Met*.. 2016;220:14–19. DOI: https://doi.org/10.1016/j.synthmet.2016.05.022
21. Geng M, Xu J, Hu S. In situ electrogenerated poly(Eriochrome black T) film and its application in nitric oxide sensor. *React. Funct. Polym*. 2008;68:1253-1259. DOI: https://doi.org/10.1016/j.reactfunctpolym.2008.06.001
22. El Attar A, Chemchoub S, Kalan MD, Oularbi L, El Rhazi M. Designing New Material Based on Functionalized Multi-Walled Carbon Nanotubes and $Cu(OH)_2$–Cu_2O/Polypyrrole Catalyst for Ethanol Oxidation in Alkaline Medium. *Front. Chem*. 2022;9:805654. DOI: https://doi.org/10.3389/fchem.2021.805654
23. Salih FE, Oularbi L, El Halim, Elbasri M, Ouarzane A, El Rhazi M. Conducting Polymer/Ionic Liquid Composite Modified Carbon Paste Electrode for the Determination of Carbaryl in Real Samples. *Electroanalysis.* 2018;30(8):1855-1864. DOI: https://doi.org/10.1002/elan.201800152
24. Mariame C, El Rhazia M, Adraoui I. Determination of traces of copper by anodic stripping voltammetry at a rotating carbon paste disk electrode modified with poly(1,8-diaminonaphtalene). *J. Anal. Chem.* 2009;64:632–636. DOI: https://doi.org/10.1134/S1061934809060161
25. Dueraning A, Kanatharana P, Thavarungkul P, Limbut W. An environmental friendly electrode and extended cathodic potential window for anodic stripping voltammetry of zinc detection. *Electrochimi*. *Acta*, 2016;221:133-143. DOI: https://doi.org/10.1016/j.electacta.2016.10.069
26. Bagheri H, Afkhami A, Khoshsafar H, Rezaei M, Shirzadmehr A. Simultaneous electrochemical determination of heavy metals using a triphenylphosphine/MWCNTs composite carbon ionic liquid electrode. *Sens. Actuators B*. 2013;186:451–460. DOI: https://doi.org/10.1016/j.snb.2013.06.051
27. Mikkelsen Ø, Schrøder KH. Sensitivity Enhancements in Stripping Voltammetry from Exposure to Low Frequency Sound. *Electroanalysis*.1999;11:401-405. DOI: https://doi.org/10.1002/(SICI)1521-4109(199905)11:6<401::AID-ELAN401>3.0.CO;2-6
28. Attar T, Harek Y, Larabi L. Determination of Ultra Trace Levels of Copper in Whole Blood by Adsorptive Stripping Voltammetry. *J. Korean Chem. Soc*.. 2013;57(5): 568-573. DOI: https://doi.org/10.5012/jkcs.2013.57.5.568
29. Moutcine A, Chtaini A. Electrochemical determination of trace mercury in water sample using EDTA-CPE modified electrode. *Sens. Bio-Sens. Res*.. 2018;17:30-35. DOI: https://doi.org/10.1016/j.sbsr.2018.01.002
30. Hassan RYA, Kamel MS, Hassan HNA, Khaled E. Voltammetric determination of mercury in biological samples using crown ether/multiwalled carbon nanotube-based sensor. *J. Electroanal. Chem.,* 2015;759:101-106. DOI: https://doi.org/10.1016/j.jelechem.2015.10.039

DEFINITIONS, ACRONYMS, ABBREVIATIONS

5-Br-PADAP: 2-(5-Bromo-2-pyridylazo)-5-diethylaminophenol
CPE: carbon paste electrode
DPASV: differential pulse anodic stripping voltammetry
EBB R: Eriochrome blue black R
EDTA: Ethylenediamine tetra-acetic acid
EPA: Environmental Protection Agency
GPE: Graphene paste electrode
Hg^{2+}: Inorganic mercury
HPLC-ICP-MS: High Performance Liquid Chromatography-inductively coupled plasma-mass spectrometry
LOD: Limit of detection
LOQ: Limit of quantification
MWCNTs: Multiwalled carbon nanotubes
RSD: relative standard deviation
EIS: Electrochemical impedance spectroscopy
UNEP: United Nation Environmental Protection
WHO: World Health Organization